Journal of Colloid and Interface Science 392 (2013) 151–157

Contents lists available at SciVerse ScienceDirect

Journal of Colloid and Interface Science

www.elsevier.com/locate/jcis

Controllable synthesis of Cu_2O petalody octahedral microcrystals and multi-patterned evolution

Yanbo Ding [a,d], Dengteng Ge [b], Lili Yang [c], Zhenyu Li [b], Wuhong Xin [b], Yao Li [b], Xiaohong Wu [d], Jiupeng Zhao [a,*]

[a] School of Chemical Engineering and Technology, Harbin Institute of Technology, Harbin 150001, China
[b] Center for Composite Materials and Structures, Harbin Institute of Technology, Harbin 150080, China
[c] School of Transportation Science and Engineering, Harbin Institute of Technology, Harbin 150090, China
[d] School of Science, Harbin Institute of Technology, Harbin 150001, China

ARTICLE INFO

Article history:
Received 9 May 2012
Accepted 25 July 2012
Available online 11 October 2012

Keywords:
Petalody octahedral
Multi-patterned
Growth mechanism
Evolution

ABSTRACT

The fabrication of cuprous oxide (Cu_2O) with various morphologies has attracted extensive interest due to its applications in solar energy conversion, electrode materials, sensors, and catalysts. Herein, we report a facile controllable route for Cu_2O microcrystals with various architectures via a hydrothermal method without using templates or surfactants. Six types of Cu_2O microcrystals including petalody octahedral, concave truncated octahedron, truncated octahedron, octahedron, sphere-like, and sphere are obtained accompanying with Cu precipitation or urchin-like CuO particles due to the modifying of pH values. The petalody octahedral pattern of Cu_2O is for the first time found here under the condition of pH 7–8. Additionally, possible growth mechanism for multi-patterned Cu_2O and compositional evolution is discussed via preferential growths induced by selective absorption of acrylic acid and decomposition of lactic acid in the present reaction system. These experimental results prove a versatile and facile strategy for Cu_2O microcrystals with special and complex architectures, which may highlights their potential applications due to the improved surface activity, catalytic, or photoelectric performance.

1. Introduction

Functional inorganic materials with unusual and novel morphologies have attracted considerable attention due to their potential applications in various fields such as solar cells, super capacitors, catalysts, medicine, electronics, and cosmetics [1–4]. Comprehensive understanding and efficient controlling of the crystal morphologies are correspondingly of dramatic importance because of the strong determination of crystal shape and texture on their properties [5]. A great number of materials with various morphologies have been reported including nanosheets/-rods/-wires/-tubes [6–10], polyhedral nanoparticles [11], hollows [12], core–shell structures [13], nanocages, and nanoframes [14]. Cuprous oxide (Cu_2O), a p-type semiconductor with direct band gap around 1.9–2.2 eV, has been regarded as one of the most promising materials for solar energy conversion [15], electrode materials [16], sensors [17], and catalysis [18]. Various methods have been devoted to the synthesis of Cu_2O nanoparticles with different morphologies, among which hydrothermal synthesis has been considered as one of the most versatile routes due to its well-controllability [19], low cost, and potential for large-scale production [20]. However, to obtain the unconventional polyhedron is still a challenge because surfaces with high reactivity usually diminish rapidly during the crystal growth process as a result of the minimization of surface energy. Thanks to the efforts from a large number of research groups, a myriad of Cu_2O micro- and nanocrystals such as nanowires [21], multipods [22], nanocubes [23], octahedra [24], and cuboctahedra [25] have been prepared with reasonable quality and quantity. It is accepted that the physical and chemical activity greatly depends on its structural parameters, such as geometry and morphology. Recently, the strategy of using organic templates and/or additives such as polyethylene glycol (PEG) or cetyl trimethyl ammonium bromide (CTAB) has been widely applied to control the morphologies of inorganic materials through the effects on nucleation and growth of inorganic particles [26,27]. However, the added templates or surfactants usually lead to the impurity of resulting materials, and the controllability of morphologies is not as well as expected.

In this paper, we report a facile and versatile hydrothermal method for synthesis of multi-patterned Cu_2O microcrystals without any assistance of templates or surfactants. This approach is involved with lactic acid as reducing agent through adjusting of which Cu or CuO with interesting morphologies was surprisingly fabricated. The morphological evolution and possible growth mechanism are also explored from the decomposition of lactic acid

* Corresponding author. Fax: +86 45186403767.
E-mail address: jiupengzhao@126.com (J. Zhao).

0021-9797/$ - see front matter © 2012 Elsevier Inc. All rights reserved.
http://dx.doi.org/10.1016/j.jcis.2012.07.095

and its property. To the best of our knowledge, Cu_2O with novel petalody octahedral or concave truncated octahedron architecture has never been reported by any chemical synthesis method. This approach highlights the potential feasibility of diverse inorganic microparticles prepared by simple hydrothermal method.

2. Experimental

All of the chemical reagents in this experiment were analytical grade and used as received without further purification. In a typical procedure, the solution consisted of 0.4 M $CuSO_4$ and 3 M lactic acid was stirred vigorously for 15 min to ensure complete dissolution. After 3 M lactic acid added into the solution, the pH of the mixture is less than 1, and a few drops of NaOH adding into the mixture for adjusting to pH 1. Then, appropriate 8 wt.% aqueous NaOH solution was added for adjusting pH values. Finally, the obtained blue solution was intensively stirred for 0.5 h at room temperature, and then, the mixed solution was transferred into a Teflon-lined stainless steel autoclave (at a pressure of 0.6–0.8 MPa, capacity 100 ml) filled up to 60% of the total volume. The autoclave was sealed and maintained at 120 °C for 14 h in an oven. After reaction, the autoclave was cooled down to room temperature naturally. The precipitates were washed with ultrapure water and anhydrous ethanol (respectively) for several times to remove residual solutions. Finally, the as-prepared products were dried at 45 °C and collected for further characterizations.

The surface morphology was performed using a QUANTA 200F SEM (FEI, American) scanning electron microscope operating at an accelerating voltage of 30 kV. The samples were sputter-coated with gold before examination. The phase composition of the crystalline structure of products was analyzed by X-ray diffraction (XRD) on a Phillips X'Pert diffractometer equipped with Cu Kα radiation at a scan rate of 5° min^{-1}.

3. Results and discussion

3.1. Phase formation of as-prepared microparticles

Full chemical environments from pH = 1 to pH = 14 were carried out to study the preparation conditions for Cu_2O microparticles. Fig. 1 shows the XRD patterns for the phase determination of the resulting particles. It is found that pure cubic phase of Cu was obtained under pH value range of 1–6 and the peaks can be clearly indexed as (111), (200), and (220) planes (JCPDS card File No. 04-0836. space group Fm-3 m (225), a_0 = 0.3615 nm). The sharp diffraction peaks indicate a high purity and crystallinity of the final product. Fig. 1b shows the XRD patterns of microparticles prepared under different alkaline conditions (pH = 7–13). All peaks can be clearly indexed as a pure cubic phase of Cu_2O and matched well with the reported data (JCPDS card File No. 05-0667. space group Pn-3 m (224), a_0 = 0.427 nm), while the different XRD pattern shown in Fig. 1c of resulting particles prepared under the condition of pH 14 is indexed as monoclinic CuO (JCPDS No. 45-0937). These results reflect that the alkali concentration plays a crucial rule in synthesis of resulting compositions.

3.2. Structure and morphology of Cu_2O microcrystal

Fig. 2 reveals the typical low- and high-magnification morphologies of resulting Cu_2O microparticles, which clearly shows an evolution of Cu_2O with several different appearances. The pattern shown in Fig. 2a could be simply described as an octahedron with each side face of petalody surfaces instead of equilateral triangles. There are several petals in each face, and the length of edge is in range of 10–15 μm. For all we know, this petalody octahedral pattern has not been found in any other reports. With the slightly increase in alkali environments, a progressive evolution is represented from petalody octahedral structure to the concave

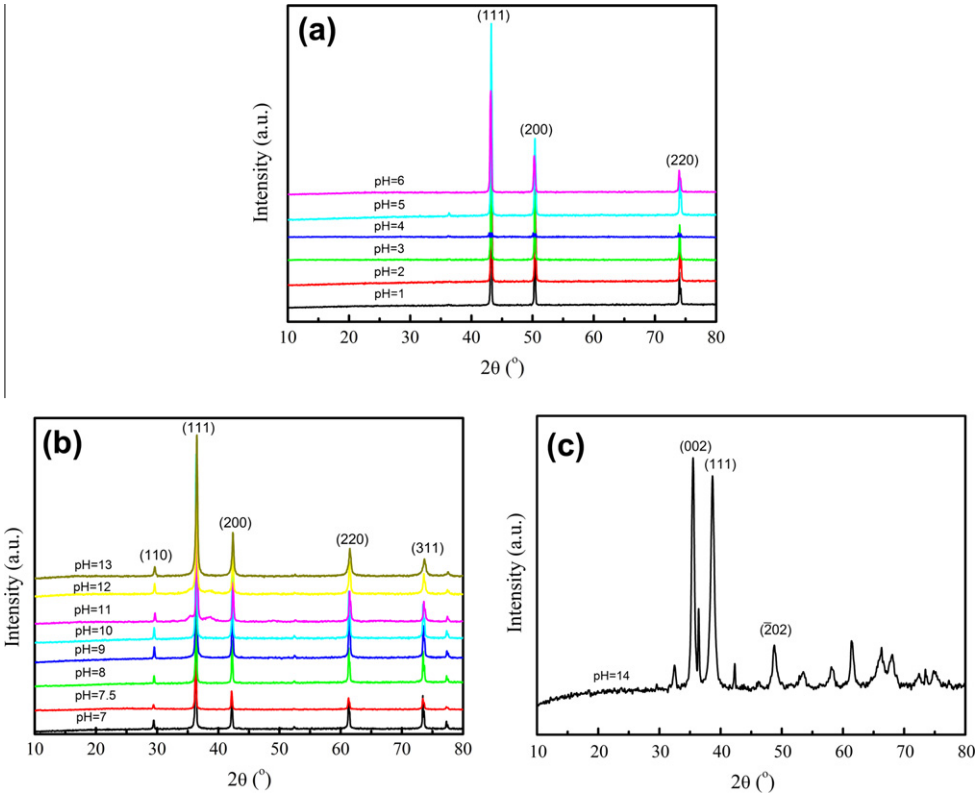

Fig. 1. XRD patterns of as-prepared microparticles synthesized at pH 1–14.

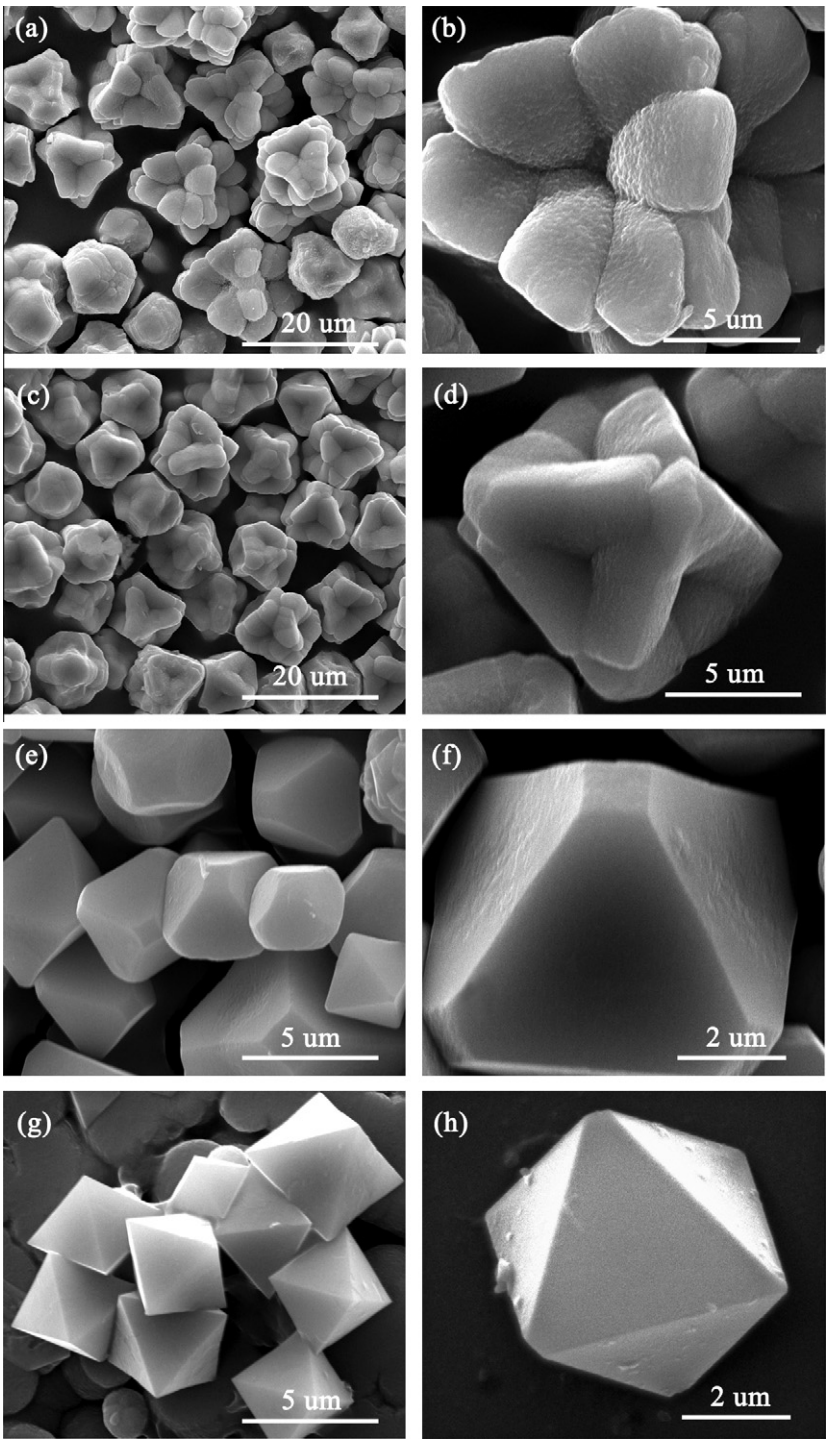

Fig. 2. SEM images of low- and high-magnification morphologies of Cu_2O microcrystals prepared under different pH values (a and b) pH = 7, (c and d) pH = 7.5, (e and f) pH = 8, (g and h) pH = 9.

truncated octahedron through each petalody faces developing into a short enclosed (Fig. 2c). The number of petals in one face is decreased, and the edge of eight faces tends to be straight and smooth, thus the length of edge is decreased to about 5–8 μm. Under the preparation condition of pH 8.0, interesting truncated octahedral Cu_2O with sharp edges was seen in Fig. 2e, which is bounded with eight trapeziform prism faces and six quadrilateral end caps with the edge length of 3–5 μm. The surface of the truncate octahedron is covered with both {1 0 0} and {1 1 1} faces, but it is mainly occupied by the {1 1 1} faces. While the {1 0 0} surfaces constantly decrease in area, concurrently, the {1 1 1} planes continually gain in area, eventually leading to perfect octahedral Cu_2O microcrystals with a length of edge to 3–4 μm when the solution adjusted to pH 9. The crystals were further grown on the basis of truncated octahedral microcrystals, which could be thought of as the framework of an octahedron, the formed crystal faces can be identified by stereological analysis of scanning electron micrographs taken from crystal samples at different viewing directions,

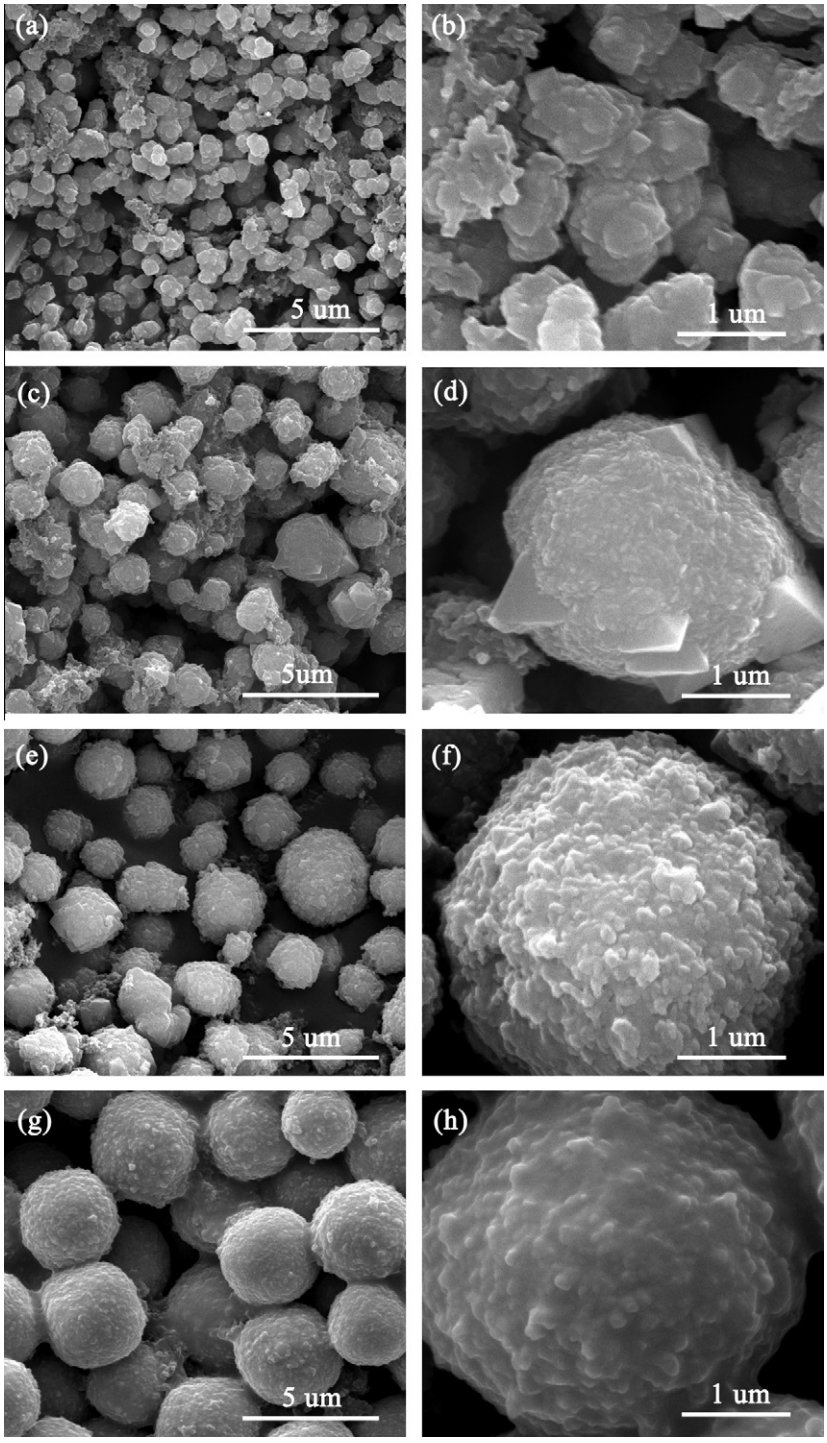

Fig. 3. SEM images of low- and high-magnification morphologies of Cu_2O microcrystals prepared under different pH values (a and b) pH = 10, (c and d) pH = 11, (e and f) pH = 12, and (g and h) pH = 13.

the morphological characteristics of {1 1 1} facets are not fully changed, and their original edges, apexes, and new edges of pits are still in the same plane.

Furthermore, quasi-sphere (Fig. 3a and c) and sphere microcrystals (Fig. 3e and g) of the Cu_2O were formed after hydrothermal treatment from pH 10–13. Cu_2O quasi-sphere particles with rough surfaces are formed with non-uniform size at the pH 10. It is obviously seen that rough Cu_2O sphere crystals constructed of distinct geometric polyhedron with the diameter ranging from 600 to 800 nm are formed (Fig. 3a). The diameter of quasi-sphere construct with several polyhedrons gets to about 1.2 μm with a further increase in volume of NaOH adding into the reaction mixture to pH 11. Notably, the spherical Cu_2O with the diameter become to 3 μm (Fig. 3e and g) can be obtained when the pH of the solution is adjusted to 12–13. Interestingly, the polyhedron disappeared and the surfaces of Cu_2O spheres become smoother, which is different from that of the quasi-sphere morphology. Moreover, the size and shape of microparticles are observed uniform and clean.

It is widely accepted that the growth process of crystals is a kinetically and thermodynamically controlled process that can

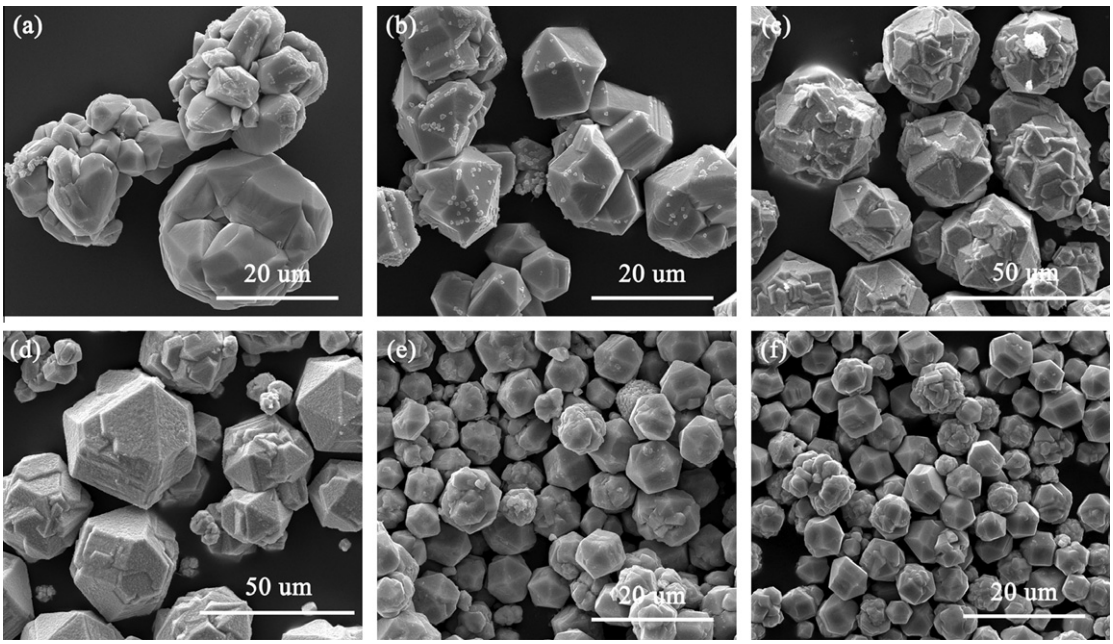

Fig. 4. SEM images of Cu microcrystals prepared under different pH values (a) pH = 1, (b) pH = 2, (c) pH = 3, (d) pH = 4, (e) pH = 5, and (f) pH = 6.

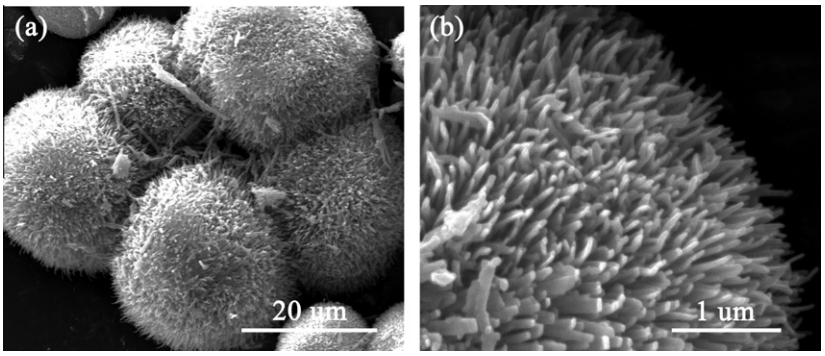

Fig. 5. SEM images of CuO microcrystals prepared under pH 14.

form different shapes with some degree of shape tunability through changes in the reaction parameters [28]. The growth mechanism will be discussed to clarify the morphology transition from petalody octahedral to sphere in the following part.

3.3. Morphologies of Cu and CuO

The resulting microparticles were proved as Cu under the acid environments by XRD results. Fig. 4 shows the low- and high-magnification SEM images of obtained Cu microparticles. A large number of irregular polyhedron structures of Cu with anisotropic polyhedral faces are exhibited. A close examination of the sample clearly reveals that the sample consists of two kinds of morphologies, one is agglomerate and the other is polyhedral, which cannot be explained by classic geometry. More interesting, an aggregation of tiny particles was formed under strong acid condition of pH 1 and pH 2. However, when more alkali adding into the solution, the surface of microcrystals reconstructs into sharp faces during the continuous growth.

The urchin-like CuO was obtained under the strong alkali condition of pH 14 as shown in Fig. 5. The diameter of a spherical assembly is up to 12 μm, which consists of many irregular strips radically pointing toward a common center. The "strips" are approximately 30–80 nm wide and more than 200 nm long. These crystal strips, analogous to the "parachutes" in a dandelion, are aligned perpendicularly to the spherical surface, which indicates that well-defined CuO urchin-like present a high surface area can be future candidates for potential application in catalysis. Considering that no additional templates are added into the formation process, the urchin-like CuO can be thought to have a habit to form this morphology due to its crystal structure (There was no separation of individual strip since they firmly assembled in the spherical structure).

3.4. Growth mechanism of $Cu/Cu_2O/CuO$

In our reaction system, the evolution of resulting product and various morphologies should be attributed to the influence of lactic acid since no surfactants/emulsions were used. It is found that $[H^+]$ or $[OH^-]$ plays an important role in the decomposition products of lactic acid such as acetaldehyde, acrylic acid, carbon monoxide, and carbon dioxide during the whole hydrothermal process [29].

Fig. 6 shows the shape evolution from Cu, Cu_2O to CuO microstructure as the reaction and pH values. Under alkali condition, Cu^{2+} appears firstly as $Cu(OH)_2$ then to a distorted $[Cu(OH)_4]^{2-}$ in the solution through edge sharing complexes with surplus OH^-

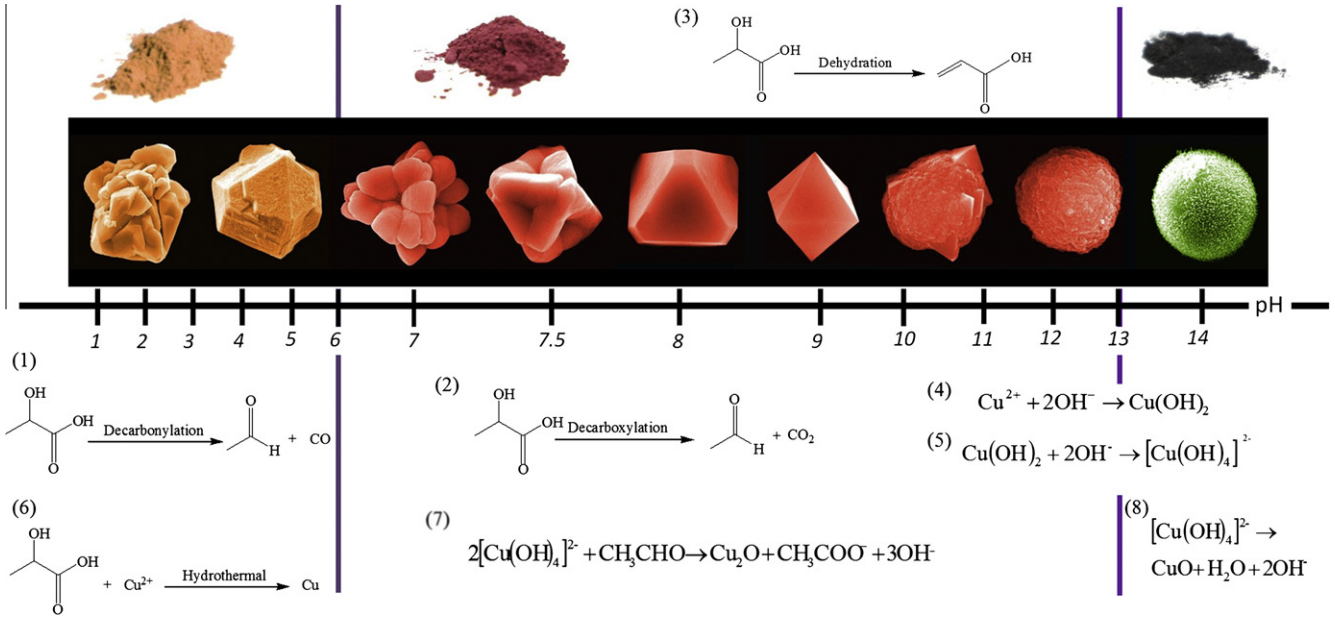

Fig. 6. Schematic illustration of the shape evolution from Cu, Cu_2O to CuO microstructures.

[30]. It has been reported [29] that the decomposition of lactic acid happens according to Eqs. (2) and (3) in Fig. 6 simultaneously, while acetaldehyde has been proved as an effective reductant under alkali condition, which generate Cu_2O as shown in Eq. (7) [31]. When more NaOH is added into the solution or other say the pH of the solution is adjusted up to 14, surplus OH^- ions are generated by the ionization of NaOH under the hydrothermal conditions. It is accepted that the $[OH^-]$ condition is less favorable for the decarbonylation of lactic acid seen as Eq. (2) [32]. In respect of the solution condition with a small amount of acetaldehyde, many researchers have reported that $[Cu(OH)_4]^{2-}$ transforms into monoclinic CuO microstructures as a result of dehydration reaction just like the Eq. (8) [33–35].

In the presence of strong acid, Gunter reported that lactic acid will decarbonizes to acetaldehyde and CO approximately under the temperature of 300 °C. In order to test the reducibility of acetaldehyde under the acid condition, we replaced the lactic acid with acetaldehyde under the same pH, time, and temperature with previous experiments. While no Cu particles were obtained, which indicate that acetaldehyde is not able to reduce Cu^{2+} to Cu. In our hydrothermal system at 120 °C, a probable mechanism for the presence of Cu is involved with an intermediate carbon-based product like CO as an excellent reductant, which favors the formation of pure metallic copper just seen as the Eq. (6). From the above discussion, it is shown that the evolution of resulting production depends on the reactions involved with lactic acid under different pH conditions.

The drastic shape tailor of Cu_2O shown in Fig. 2 is also an interesting and meaningful phenomenon. In the past several years, systematic control of Cu_2O including morphology, crystallinity, and structure has been reported through external agent [36]. Sun and his co-workers [37] reported that selective adsorption of ethanol molecules on different positions of Cu_2O octahedral particles leaded to a designated tailoring on {1 1 1} facet to synthesize etching-limited branching architectures. It is indicated that the preferential adsorption of capping agent in solution to different crystal facets determines the formation of various morphologies. In our system under the pH range of 7–13, the capping agent here should be the acrylic acid, which is also produced through Eq. (3) accompany with Eq. (2) under the alkali condition. The introduced acrylic acid molecules prefer to adsorb onto the higher energy surfaces during the crystal growth. The adsorption stabilizes the facets and thus hinders the growth rate perpendicular to it, which changes the growth rates of different crystal directions, it is also induces the surface energy rearrangement of each face of the Cu_2O. This leads to the exposure of the large {1 1 1} surfaces and the formation of the final Cu_2O microcrystal. Thus, these new morphologies of Cu_2O crystals could form under a kinetic growth regime; however, it is still remains a great challenge to exploit a facile route to understand the growth habit of {1 1 1} facets and achieve the well-defined different morphology of Cu_2O growth on {1 1 1} facets.

The strong alkali used in the above precipitation reaction played a vital role during the synthesis based on the experimental results. The high concentration of $[Cu(OH)_4]^{2-}$ in the whole reaction process due to the strong alkaline media accelerates the dehydration of $[Cu(OH)_4]^{2-}$, which leads to the high quantity of CuO nuclei according to Eqs. (4), (5) and (8). The formation process of CuO urchin-like microcrystalline can be expressed as follows: $[Cu(OH)_4]^-$ was hydrolyzed to CuO nuclei via hydrothermal treatment and the small CuO nuclei were assembled into microparticles under acrylic acid adsorption at the high energy faces. The formation of urchin-like CuO nanostructures was controlled by the kinetics under the high concentration of NaOH.

4. Conclusions

In summary, we showed a simple hydrothermal method for the preparation of well-controlled Cu_2O microcrystals with novel morphologies and transformation to Cu or CuO by adjusting pH conditions. The micropattern of petalody octahedral and concave truncated octahedron Cu_2O was firstly reported here under the condition of pH 7–8. The Cu_2O morphologies evolve from petalody octahedral, concave truncated octahedron to truncated octahedron, octahedron, sphere-like and ultimately to sphere strongly show the dependence on increased alkali condition. The possible growth mechanism of all kinds of microcrystals has been discussed in terms of a preferential growths induced by selective absorption of acrylic acid. Moreover, the Cu precipitation and urchin-like CuO

were also formed under the acid or strong alkali condition due to the different decomposition of lactic acid in the present reaction system. These results reported here provide a facile pathway for novel multi-morphologic Cu_2O microcrystals with well-controllability. Further works on the special characteristic and applications of these microcrystals will be involved including the possibilities of improving performance based on Cu_2O electrodes in photovoltaic, sensors, and battery applications.

Acknowledgments

This work is supported by the Program National Natural Science Foundation(Nos. 51010005, 51174063and 51102068), the Program for New Century Excellent Talents in University (NCET-08-0168), and Sino-German joint project (GZ550).

References

[1] S. Mann, Int. Ed. 39 (2000) 3392–3406.
[2] J.S. Xu, D.F. Xue, J. Phys. Chem. B 109 (2005) 17157–17161.
[3] X. Duan, Y. Huang, R. Agarwal, C.M. Lieber, Nature 421 (2003) 241–245.
[4] J. Goldberger, R. He, Y. Zhang, S. See, H. Yang, H.J. Choi, P. Yang, Nature 422 (2003) 599–602.
[5] S. Piana, M. Reyhani, J.D. Gale, Nature 438 (2005) 70–73.
[6] E.S. Jang, J.H. Won, Y.W. Kim, X.Y. Chen, J.H. Choy, Cryst. Eng. Commun. 12 (2010) 3467.
[7] S. Zhu, H. Zhou, M. Hibino, I. Honma, M. Ichihara, Adv. Funct. Mater. 15 (2005) 381–386.
[8] L. Guo, Y.L. Ji, H.B. Xu, J. Am. Chem. Soc. 124 (2002) 14864–14865.
[9] M.J. Siegfried, K.S. Choi, J. Am. Chem. Soc. 128 (2006) 10356–10357.
[10] Y.W. Tan, X.Y. Xue, Q. Peng, H. Zhao, T.H. Wang, Y.D. Li, Nano Lett. 7 (2007) 3723–3728.
[11] D.F. Zhang, H. Zhang, L. Guo, K. Zheng, X.D. Han, Z. Zhang, J. Mater. Chem. 19 (2009) 5220–5225.
[12] M. Diab, B. Moshofsky, I.J.L. Plante, T. Mokari, J. Mater. Chem. 21 (2011) 11626–11631.
[13] C.H. Kuo, Y.C. Yang, S. Gwo, M.H. Huang, J. Am. Chem. Soc. 133 (2011) 1052–1057.
[14] C.H. Kuo, M.H. Huang, J. Am. Chem. Soc. 130 (2008) 12815–12820.
[15] A. Musa, T. Akomolafe, M. Carter, Sol. Energy Mater. Sol. Cells 51 (1998) 305–316.
[16] P. Poizot, S. Laruelle, S. Grugenon, L. Dupont, J. Taracon, Nature 407 (2000) 496–499.
[17] J. Zhang, J. Liu, Q. Wang, X. Li, Chem. Mater. 18 (2006) 867–871.
[18] B. White, M. Yin, A. Hall, D. Le, S. Stolbov, T. Rahman, N. Turro, S. O' Brien, Nano Lett. 6 (2006) 2095–2098.
[19] M. Yang, H.P. You, Y.H. Zheng, K. Liu, G. Jia, Y.H. Song, Y.J. Huang, L.H. Zhang, H.J. Zhang, Inorg. Chem. 48 (2009) 11559–11565.
[20] C. Lu, L. Qi, J. Yang, D. Zhang, N. Wu, J. Ma, J. Phys. Chem. B 108 (2004) 17825–17829.
[21] X.L. Deng, S. Hong, I. Hwang, J.S. Kim, J.H. Jeon, Y.C. Park, J.J. Lee, S.O. Kang, T. Kawai, B.H. Park, Nanoscale 4 (2012) 2029–2033.
[22] Y. Chang, H.C. Zeng, Cryst. Growth Des. 4 (2004) 273–278.
[23] F. Hong, S.D. Sun, H.J. You, S.C. Yang, J.X. Fang, S.W. Guo, Z.M. Yang, B.J. Ding, X.P. Song, Cryst. Growth Des. 11 (2011) 3694–3697.
[24] C.H. Kou, M.H. Huang, J. Am. Chem. Soc. 130 (2008) 12815–12820.
[25] D.F. Zhang, H. Zhang, L. Guo, K. Zheng, X.D. Han, Z. Zhang, J. Mater. Chem. 19 (2009) 5220–5226.
[26] W.Z. Wang, G.H. Wang, X.S. Wang, Y.J. Zhan, Y.K. Liu, C.L. Zheng, Adv. Mater. 14 (2002) 67–69.
[27] H.W. Zhang, X. Zhang, H.Y. Li, Z.K. Qu, S. Fan, M.Y. Ji, Cryst. Growth Des. 7 (2007) 820–824.
[28] Z.W. Quan, C.X. Li, X.M. Zhang, J. Yang, P.P. Yang, C.M. Zhang, J. Lin, Cryst. Growth Des. 8 (2008) 2384–2392.
[29] W.S. Mok, M.J. Antal Jr., J. Org. Chem. 54 (1989) 4596–4602.
[30] O. Akhavan, R. Azimirad, S. Safa, E. Hasani, J. Mater. Chem. 21 (2011) 9637–9643.
[31] K. Leung, P.J. Huang, Y.C. Chena, C.M. Lee, J. Chin. Chem. Soc. 58 (2011) 655–659.
[32] S. Varadarajan, D.J. Miller, Biotechnol. Prog. 15 (1999) 845–854.
[33] H. Cao, C.W. Hu, Y.H. Wang, Y.H. Guo, C.X. Guo, E.B. Wang, Chem. Commun. 15 (2003) 1884–1885.
[34] L.F. Gou, C.J. Murphy, J. Mater. Chem. 14 (2004) 735–738.
[35] X.J. Zhang, J. Phys. Chem. C 112 (2008) 16847–16851.
[36] Z. Qin, Y.H. Huang, Q.Y. Wang, J.J. Qi, X.J. Xing, Y. Zhang, Cryst. Eng. Commun. 12 (2010) 4156–4160.
[37] S.D. Sun, H.J. You, C.C. Kong, Cryst. Eng. Commun. 13 (2011) 2837–2840.